Joint 48th IEEE Conference on Decision and Control and
28th Chinese Control Conference
Shanghai, P.R. China, December 16-18, 2009

A Robust STATCOM Control to Augment LVRT capability of Fixed Speed Wind Turbines

M. J. Hossain, H. R. Pota, V. Ugrinovskii, Senior Member, IEEE and Rodrigo A. Ramos, Senior Member, IEEE

Abstract— **In this paper, we propose an algorithm to design a robust output feedback controller for a Static Synchronous Compensator (STATCOM) to enhance the Low-Voltage Ride-Through (LVRT) capability of fixed-speed wind turbines equipped with induction generators. The wind generator is a highly nonlinear system, and in this paper it is modelled as a linear part plus a nonlinear part. The nonlinear part is written as the Cauchy remainder term in Taylor series expansion; this enables us to use the bound of this term in robust control design. Large disturbance simulations demonstrate that the proposed controller enhances voltage stability as well as transient stability of induction generators during low voltage ride through transients and thus enhances the LVRT capability.**

I. Introduction

Wind energy has emerged as the fastest growing source of energy and is expected to see continued strong growth in the immediate future. Most interconnection standards today require wind farms to have the ability to ride through faults. The low voltage ride through requirement basically demands that the wind farm remains connected to the grid for voltage level as low as 5% of the nominal voltage for up to 140 ms [3].

Induction generators are preferred as wind generators for their low cost and maintenance due to rugged brushless construction. Constant speed wind turbines equipped with induction generators have the advantage of not having power electronics on board and they are used widely in offshore wind farms [2]. Although the use of variable-speed wind turbines with power electronic interfaces is the trend, many directly connected induction-generator-based wind turbines are still in operation. These induction generators by themselves are not able to contribute to power system regulation and control in the same way as a conventional field excited synchronous generator. Induction generators need reactive power support to be connected to stiff grids. However, wind turbines are usually connected at weak nodes or at distribution levels where the network was not originally designed to transfer power into the grid. This increases the need for dynamic reactive power support to ride-through severe faults.

This work was supported by the Australian Research Council and the University of New South Wales at the Australian Defence Force Academy.

M. J. Hossain, H. R. Pota, V. Ugrinovskii are with the school of ITEE, UNSW@ADFA, Canberra, ACT-2600, Australia (m.hossain,h.pota,v.ougrinovski)@adfa.edu.au

R. A. Ramos is with the Dept. of Electrical Engg., Engineering School of São Carlos, Brazil (ramos@sel.eese.usp.br).

Squirrel cage induction generator consumes reactive power and it slows down voltage restoration after a fault. This can lead into voltage and rotor-speed instability. During a fault, the generator will accelerate due to the imbalance between the mechanical power extracted from the wind and electrical power delivered to the grid. When the voltage is restored after the fault is cleared the generator will consume reactive power, impeding the voltage restoration. When the voltage does not rise quickly enough, the generator continues to accelerate and consumes even larger amount of reactive power. This process may eventually lead to voltage and rotor-speed instability and more so if the wind turbine is connected to a weak grid. To prevent these types of instabilities, advanced and faster STATCOM controllers can be connected to the system.

STATCOM technology adds the missing functionality to wind parks in order to become grid code compliant. The fast dynamic voltage control and the behavior of STATCOM during balanced or unbalanced grid faults (fault ride through), allow wind generators to meet the stringent grid code requirements. The application of STATCOMs for stabilising wind generators is reported in [12], [15]. The authors in [12] have analysed the extent to which the low voltage ride through (LVRT) capability of wind farms using squirrel cage generators can be enhanced by the use of a STATCOM with conventional control, compared to the thyristor controlled static Var compensator (SVC).

Linear control techniques have been predominantly used for controlling a STATCOM. In this approach the system equations are linearized around an operating point. Based on this linearized model, the conventional proportional-integral (PI) controllers are fine tuned to effectively respond to the small scale and large scale disturbances in the power system, where the STATCOM is connected. For instance PI controllers are used in STATCOMs to design internal controllers for distribution which enables them to mitigate voltage flicker [19]. While these models are appropriate for certain small signal applications in the vicinity of a specific steady state operating point, they cannot capture the true nature of the power network and the STATCOM when the system is exposed to large scale faults or dynamic disturbances that change the configuration of the plant to be controlled.

The authors in [8] propose a proportional-integral-derivative (PID) pitch angle controller for a fixed speed active-stall wind turbine. The controller is designed using

978-1-4244-3872-3/09/$25.00 ©2009 IEEE

root-locus method and the nonlinearities of the system are taken into account to determine the second-order transfer functions using step response which represents the system more accurately compared to linear representation. The actual transfer function of the wind turbines is of higher order and the method in [8] cannot capture nonlinearity accurately. To capture the nonlinearity fully, a method using mean-value theorem is proposed in [6] and a excitation controller is designed where unstructured uncertainty representation is presented. This representation is simplified but conservative.

The STATCOM with a voltage or current source converter is a nonlinear device. The converter model is usually a multi-input multi-output nonlinear system. The difficulty in controlling the converter is mainly due to the nonlinearity. There are several ways of dealing with the nonlinearity. The simplest way is to use two PI controllers to control the DC term and the reactive power separately [7]. However, in these cases, the response time is usually large, and it is difficult to find appropriate PI parameters in a systematic way. Another method is to write the state equations of the system, then linearize the system around an operating point [18]. The problem with this method is that the controller design is dependent on the operating point, which is not adequate in the event of large disturbances.

This paper presents a sophisticated method for dealing with nonlinearity using a linearisation method where the Cauchy remainder is included in the design process as bounded uncertainty. The mean-value theorem allows to retain system nonlinearities in the system model; this improves modelling accuracy for representing nonlinear dynamics. This reformulation allows us to design a robust controller against structured uncertainty, which refers to the fact that the uncertainty can be broken up into a number of independent uncertainty blocks. Finally, a robust output feedback linear STATCOM controller is designed to enhance the LVRT capability of wind generators. The controller performance is evaluated through nonlinear simulations by applying large disturbances. The comparisons of these results with those obtained from conventional PI-based STATCOM controller [16] reveals the efficacy of the proposed STATCOM control design.

The organization of the paper is as follows: Section II provides the mathematical modelling of the power system devices under consideration, and test system and control task are presented in Section III. Section IV describes the linearisation technique and bounding for uncertainties and Section V discusses the STATCOM controller design technique. Controller design algorithm and performance of the controller are outlined in Section VI. Section VII draws the conclusion.

II. Power System Model

The wind speed and mechanical power extracted from the wind are related as [1]:

$$P_{wti} = \frac{\rho_i}{2} A_{wti} c_{pi}(\lambda_i, \theta_i) V_{wi}^3, \tag{1}$$

where P_{wti} is the power extracted from the wind in watts, ρ_i is the air density (kg/m^3), c_{pi} is the performance coefficient or power coefficient, tip speed ratio $\lambda_i = \frac{\omega_{wti} R_i}{V_{wi}}$, R_i is the wind turbine radius (m), ω_{wti} is the wind turbine rotational speed (rad/s), V_{wi} is the wind speed (m/s), θ_i is the pitch angle (degree) and A_{wti} is the area covered by the wind turbine rotor (m^2).

For representation of fixed-speed induction generator models in power system stability studies [4], the stator flux transients can be neglected in the voltage relations. A simplified transient model of a single cage induction generator with the stator transients neglected and rotor currents eliminated, is described by the following differential equations [1], [13]:

$$\dot{s}_i = \frac{1}{2H_{mi}} \left[T_{mi} - T_{ei} \right], \tag{2}$$

$$\dot{E}'_{qri} = -\frac{1}{T'_{oi}} \left[E'_{qri} - (X_i - X'_i) i_{dsi} \right] - s_i \omega_s E'_{dri}, \tag{3}$$

$$\dot{E}'_{dri} = -\frac{1}{T'_{oi}} \left[E'_{dri} + (X_i - X'_i) i_{qsi} \right] + s_i \omega_s E'_{qri}, \tag{4}$$

$X'_i = X_{si} + X_{mi} X_{ri} / (X_{mi} + X_{ri})$, is the transient reactance, $X_i = X_{si} + X_{mi}$, is the rotor open-circuit reactance, $T'_{oi} = (L_{ri} + L_{mi})/R_{ri}$, is the transient open-circuit time constant, $P_{si} = V_{dsi} i_{dsi} + V_{qsi} i_{qsi}$, is the real power, $Q_{si} = V_{qsi} i_{dsi} - V_{dsi} i_{qsi}$, is the reactive power, $V_{ti} = \sqrt{V_{dsi}^2 + V_{qsi}^2}$, is the terminal voltage of induction generator, s_i is the slip, E'_{dri} is the direct-axis transient voltage, E'_{qri} is the quadrature-axis transient voltage, V_{dsi} is the d-axis stator voltage, V_{qsi} is the q-axis stator voltage, T_{mi} is the mechanical torque, T_{ei} is the electrical torque, X_{si} is the stator reactance, X_{ri} is the rotor reactance, X_{mi} is the magnetizing reactance, R_{si} is the stator resistance, R_{ri} is the rotor resistance, H_{mi} is the inertia constant of the generator, $\delta_i = \int_0^t \omega_{ri} dt$, is the rotor angle, ω_{ri} is the rotor speed, ω_s is the synchronous speed, i_{dsi} and i_{qsi} are d- and q-axis components of stator current, respectively.

Basic STATCOM circuit consists of a voltage source converter (VSC) and a dc capacitor. The dynamic of this voltage source is governed by the charging and discharging of a large (nonideal) capacitor. The capacitor voltage can be adjusted by controlling the phase angle difference between line voltage V_t and VSC voltage E. If the phase angle of line voltage is taken as a reference, the phase angle of VSC voltage is the same as the firing angle α of VSC. Thus, if the firing angles are slightly advanced, the dc voltage V_{dc} decreases, and reactive power flows into STATCOM. Conversely, if the firing angles are slightly delayed, the dc voltage increases and STATCOM supplies reactive power to the bus. By controlling the firing angles of VSC, the reactive power can be generated from or absorbed by STATCOM and thus the voltage regulation can be achieved. The STATCOM model can be described by the following equation:

$$\dot{V}_{dc}(t) = -\frac{P_s}{C V_{dc}} - \frac{V_{dc}}{R_c C}, \tag{5}$$

where V_{dc} is the capacitor voltage, P_s is the power supplied by the system to the STATCOM to charge the capacitor, which is a nonlinear function of

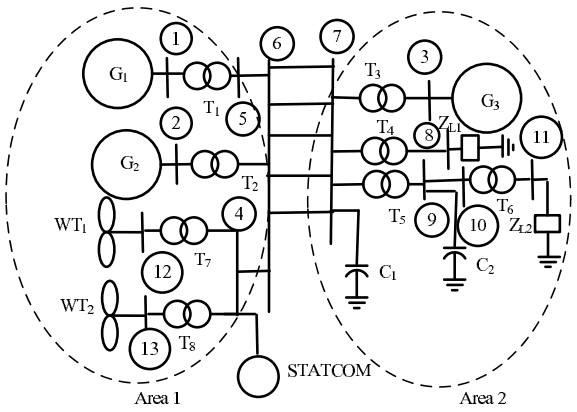

Fig. 1. Power System Model.

$(\alpha, k, E, V_{dc}, E'_{qr}, E'_{dr}$, and $E = kV_{dc}\angle\alpha)$. The control inputs are related to V_{dc} through P_s. The STATCOM bus voltage measurement system is modelled as a first order system (for constants T_m and K_m):

$$\dot{v}_{tm} = -\frac{v_{tm}}{T_m} + K_m V_t, \tag{6}$$

where v_{tm} is the sensor output and V_t is the voltage at Bus 4. For stability analysis we include the transformer and the transmission line in the reduced admittance matrix.

III. Test System and Control Task

The test system shown in Fig. 1 consists of 11 buses and 3 generators. The parameters for the system are given in [10]. The total load for this system is $P_L = 6655$ MW and $Q_L = 2021$ MVAr and the generation is $P_G = 6871$ MW, $Q_G = 1738$ MVAr. The generation in a remote area (generators $G_1 = 3981$ MW, and $G_2 = 1736$ MW) is connected to the main load through five transmission lines. The remaining load (P=1154 MW) is supplied by the local generator, G_3. The load at Bus 11 is modelled as 50% constant impedance and 50% constant current for both active and reactive power and the load at bus 8 is modelled as constant MVA for both active and reactive power.

We design a robust STATCOM controller for the modified test system where the generators $G_2 = 0$ MW, $G_3 = 0$ MW, $WT_1 = 1736$ MW, and $WT_1 = 1154$ MW. The remaining power is supplied from G_1 which is considered in this paper as an infinite bus. A STATCOM is connected at Bus 4 to meet the connection requirements for power system grids. The wind generators are arranged in two parallel lines and we represent each of them by an aggregated wind generator model [5]. To appreciate the nature of the control task, we carry out the modal analysis for the open loop system. The dominant mode for the test system is $-0.105 \pm j0.71$. The participation vector for the dominant mode is shown in Table I. The participation vector indicates that the states E'_{qr1}, E'_{qr2}, s_1 and s_2 have the most significant contribution to the dominant mode. The dominant mode is related to both reactive and active power mismatch. The reactive power can be controlled by the designed STATCOM controller and a conventional pitch controller is used to control real power,

TABLE I
Participation Factors

States	$\triangle s_1$	$\triangle E'_{dr1}$	$\triangle E'_{qr1}$	$\triangle s_2$	$\triangle E'_{dr2}$	$\triangle E'_{qr2}$
Parti. Factor	0.96	0.048	1.0	0.94	0.04	0.97

which uses slip as the input [1]. For the test system, the state vector is $x = \left[s_1, E'_{dr1}, E'_{qr1}, s_2, E'_{dr2}, E'_{qr2}, V_{dc}, V_{tm}\right]^T$.

IV. Linearisation and Uncertainty Modelling

Linear controllers are designed based on the Taylor series approximation around an equilibrium point. This linearisation technique limits the applicability of the linear model to small deviations from the equilibrium point. In general, the range of these small deviations is difficult to quantify. To quantify the neglected higher order terms, we propose the use of a linearisation scheme which retains the contributions of the higher order terms in the form of the Cauchy remainder. In the design of the linear controller, a bound on the Cauchy remainder is incorporated as an uncertain term thus quantifying the deviations permitted in the linear model.

Let (x_0, u_0) be an arbitrary point in the control space, using the mean-value theorem, the test system dynamics can be rewritten as follows [9]:

$$\dot{x} = f(x_0,u_0) + L(x-x_0) + M(u-u_0), \tag{7}$$

$$\text{where} \quad L = \left[\left.\frac{\partial f_1}{\partial x}\right|_{\substack{x=x^{*1}\\u=u*1}}, \ldots, \left.\frac{\partial f_8}{\partial x}\right|_{\substack{x=x^{*8}\\u=u*8}}\right]^T,$$

$$M = \left[\left.\frac{\partial f_1}{\partial u}\right|_{\substack{x=x^{*1}\\u=u*1}}, \ldots, \left.\frac{\partial f_8}{\partial u}\right|_{\substack{x=x^{*8}\\u=u*8}}\right]^T.$$

Here (x^{*p}, u^{*p}) , $p = 1, \cdots, 8$, denote points lying on the line segment connecting (x,u) and (x_0,u_0) and $f = [f_1, \ldots, f_8]^T$ denotes the vector function on the right-hand side of the vector differential equations. The identity in equation (7) is an exact reformulation of the system. The nonlinearity of the system is captured through the nonlinear dependencies $x^{*p} = \Phi_p(x,u,x_0,u_0)$ and $u^{*p} = \Psi_p(x,u,x_0,u_0)$, $\quad p = 1, \ldots, 8$.

Letting (x_0,u_0) be the equilibrium point about which the trajectory is to be stabilized and defining $\Delta x \triangleq x - x_0$, $\Delta u \triangleq u - u_0$, it is possible to rewrite (7) as follows:

$$\begin{aligned}\Delta\dot{x} &= \dot{x} - \dot{x_0} = L(x-x_0) + M(u-u_0),\\ &= A\triangle x + (L-A)\triangle x + B_1\triangle u + (M-B_1)\triangle u,\end{aligned} \tag{8}$$

where $A = \left.\frac{\partial f}{\partial x}\right|_{\substack{x=x_0\\u=u_0}}$ and $B_1 = \left.\frac{\partial f}{\partial u}\right|_{\substack{x=x_0\\u=u_0}}$.

We rewrite system (8) in terms of the block diagram shown in Fig. 2. Let

$$(L-A)\triangle x + (M-B_1)\triangle u = \sum_{k=0}^{7} B_{2k}\xi_k(t), \tag{9}$$

where $\xi_1(t), \ldots, \xi_k(t)$ are known as the uncertainty inputs. The matrices $[B_{20}, \cdots, B_{27}]$, $\left[\tilde{C}_{10}, \cdots, \tilde{C}_{27}\right]$ and $\left[\tilde{D}_{10}, \cdots, \tilde{D}_{27}\right]$ are calculated such that

$$(L-A)\triangle x + (M-B_1)\triangle u =$$

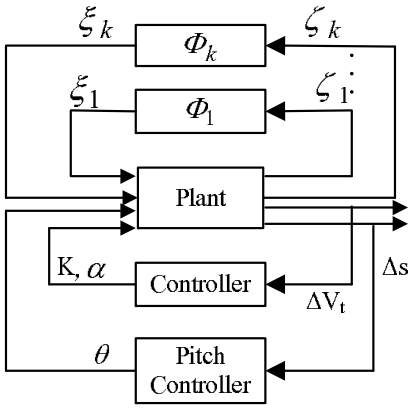

Fig. 2. Control Strategy.

$$\sum_{k=0}^{7} B_{2k}\tilde{\phi}_k(t)\tilde{C}_{1k}\triangle x + \sum_{k=0}^{7} B_{2k}\tilde{\psi}_k(t)\tilde{D}_{1k}\triangle u \qquad (10)$$

where $\xi_k = \tilde{\phi}_k\tilde{C}_{1k}\triangle x + \tilde{\psi}_k\tilde{D}_{1k}\triangle u$, $k = 0,\ldots,7$, and

$$B_{20} = \begin{bmatrix} \frac{1}{2H_{m1}} & 0 & 0 & 0 & 0 & 0 & 0 & 0 \end{bmatrix}^T,$$
$$B_{21} = \begin{bmatrix} 0 & \frac{T'_{01}}{X_1 - X'_1} & 0 & 0 & 0 & 0 & 0 & 0 \end{bmatrix}^T,$$
$$B_{22} = \begin{bmatrix} 0 & 0 & \frac{T'_{01}}{X_1 - X'_1} & 0 & 0 & 0 & 0 & 0 \end{bmatrix}^T,$$
$$B_{23} = \begin{bmatrix} 0 & 0 & 0 & \frac{1}{2H_{m2}} & 0 & 0 & 0 & 0 \end{bmatrix}^T,$$
$$B_{24} = \begin{bmatrix} 0 & 0 & 0 & 0 & \frac{T'_{02}}{X_2 - X'_2} & 0 & 0 & 0 \end{bmatrix}^T,$$
$$B_{25} = \begin{bmatrix} 0 & 0 & 0 & 0 & 0 & \frac{T'_{02}}{X_2 - X'_2} & 0 & 0 \end{bmatrix}^T,$$
$$B_{26} = \begin{bmatrix} 0 & 0 & 0 & 0 & 0 & 0 & \frac{1}{To1} & 0 \end{bmatrix}^T,$$
$$B_{27} = \begin{bmatrix} 0 & 0 & 0 & 0 & 0 & 0 & 0 & K_m X_{s1} \end{bmatrix}^T,$$
$$\tilde{C}_{1k} = \begin{bmatrix} 1 & 0 & 0 & 0 & 0 & 0 & 0 & 0 \\ 0 & 1 & 0 & 0 & 0 & 0 & 0 & 0 \\ 0 & 0 & 1 & 0 & 0 & 0 & 0 & 0 \\ 0 & 0 & 0 & 1 & 0 & 0 & 0 & 0 \\ 0 & 0 & 0 & 0 & 1 & 0 & 0 & 0 \\ 0 & 0 & 0 & 0 & 0 & 1 & 0 & 0 \\ 0 & 0 & 0 & 0 & 0 & 0 & 1 & 0 \end{bmatrix},$$
$$\tilde{D}_{1k} = \begin{bmatrix} 1 & 1 & 1 & 1 & 1 & 1 & 1 & 1 \\ 1 & 1 & 1 & 1 & 1 & 1 & 1 & 1 \end{bmatrix}^T,$$

$k = 0,\ldots,7$. The expressions for obtaining $\tilde{\phi}_k(t)$ and $\tilde{\psi}_k(t)$ are not given in this paper due to space limitation. This can be downloaded from http://www.ee.adfa.edu.au/staff/hrp/CDC09phi.pdf.

The system can now be written as

$$\triangle\dot{x} = A\triangle x + B_1\triangle u + \sum_{k=0}^{7} B_{2k}\xi_k(t). \qquad (11)$$

We define $C_{1k} = \sqrt{\beta_k}\tilde{C}_{1k}$, and $D_{1k} = \sqrt{\beta_k}\tilde{D}_{1k}$, where β_k are scaling factors which affect the magnitude of the uncertain outputs ζ_k, $k = 0,\ldots,7$.

We write $\phi_k(t) = \frac{1}{\sqrt{\beta_k}}\begin{bmatrix}\tilde{\phi}_k(t) & \tilde{\psi}_k(t)\end{bmatrix}$. We choose β_k such that

$$\|\phi_k(t)\|^2 \le 1,\ k = 0,\ldots,7. \qquad (12)$$

With these values of β_k, we can conclude that for the values (Section 6) of s_i^*, E_{dri}^*, E_{qri}^*, δ_i^*, V_{dc}^*, and V_{tm}^*, $i = 1,2$,

$$\|\xi_k(t)\|^2 \le \beta_k\|\left(\tilde{C}_{1k}\triangle x + \tilde{D}_{1k}\triangle u\right)\|^2. \qquad (13)$$

We also define $\zeta_k = \sqrt{\beta_k}\left(\tilde{C}_{1k}\triangle x + \tilde{D}_{1k}\triangle u\right)$. From this we recover the IQC (integral quadratic constraint) [14],

$$\|\xi_k(t)\|^2 \le \|\zeta_k(t)\|^2,\ k = 0,\ldots,7 \qquad (14)$$

To facilitate control design, the power system model is finally summarized as

$$\triangle\dot{x}(t) = A\triangle x(t) + B_1\triangle u(t) + \sum_{k=0}^{7} B_{2k}\xi_k(t), \qquad (15)$$

$$y(t) = C_2\triangle x(t) + \sum_{k=0}^{7} D_{2k}\xi_k(t)), \qquad (16)$$

$$\zeta_k(t) = C_{1,k}\triangle x(t) + D_{1,k}u(t),\ k = 0,\ldots,7 \qquad (17)$$

where ζ_k, $k = 0,\ldots,7$, are known as the uncertainty outputs and $y(t)$ is the measured output.

The output matrix is defined as $C_2 = \begin{bmatrix}0,0,0,0,0,0,0,1\end{bmatrix}$. We choose $D_{20} = 0.01$, $D_{21} = 0.01$, $D_{22} = 0.01$, $D_{23} = 0.1$, $D_{24} = 0.1$, $D_{25} = 0.01$, $D_{26} = 0.1$, $D_{27} = 0.005$. Equations (15)–(17) provide a new representation of the power system model which contains the linear part, and also another part with higher order terms. The new formulation presented in this section is used to design a robust output feedback STATCOM controller for the nonlinear power system.

V. Robust Statcom Control

The control design problem considered in this paper is of providing a stabilising robust output feedback control algorithm for a system containing structured uncertainty described by a certain IQC (Integral Quadratic Constraint) [14], [17]. The output feedback control method is applied to the uncertain systems of the form shown in Fig. 2.

It is shown in [17] that the linear robust control theory can be applied to (15)–(17) subject to the following constraint:

$$\int_0^{t_i}\|\xi_k(t)\|^2 dt \le \int_0^{t_i}\|\zeta_k(t)\|^2 dt,\ \forall i \text{ and } \forall k = 0,\ldots,7. \quad (18)$$

The necessary and sufficient condition for the absolute stabilisability of the uncertain system (15)-(17) is given in terms of the existence of solution to a pair of parameter dependent algebraic Riccati equations [14]. The Riccati equations under consideration are defined as follows: for given constants $\tau_1 > 0,\ldots,\tau_7 > 0$;

$$(A - \tilde{B}_2\tilde{D}_2^T\Gamma_\tau^{-1}C_2)Y + Y(A - \tilde{B}_2\tilde{D}_2^T\Gamma_\tau^{-1}C_2)^T + Y(C_\tau^T C_\tau - C_2^T\Gamma_\tau^{-1}C_2)Y + \tilde{B}_2(I - \tilde{D}_2^T\Gamma_\tau^{-1}\tilde{D}_2)\tilde{B}_2^T = 0, \qquad (19)$$

$$X(A - B_1G_\tau^{-1}D_\tau^T C_\tau) + (A - B_1G_\tau^{-1}D_\tau^T C_\tau)^T X + C_\tau^T (I - D_\tau G_\tau^{-1}D_\tau^T)C_\tau + X(\tilde{B}_2\tilde{B}_2^T - B_1G_\tau^{-1}B_1^T)X = 0, \qquad (20)$$

$$C_\tau = \begin{bmatrix} C_{10} \\ \sqrt{\tau_1}C_{11} \\ \vdots \\ \sqrt{\tau_7}C_{17} \end{bmatrix}; \quad D_\tau = \begin{bmatrix} D_{10} \\ \sqrt{\tau_1}D_{11} \\ \vdots \\ \sqrt{\tau_7}D_{17} \end{bmatrix};$$

$$\tilde{B}_2 = \begin{bmatrix} B_{20} & \frac{1}{\sqrt{\tau_1}}B_{21} & \cdots & \sqrt{\tau_7}B_{27} \end{bmatrix}; \quad G_\tau = D_\tau^T D_\tau;$$

$$\tilde{D}_2 = \begin{bmatrix} D_{20} & \frac{1}{\sqrt{\tau_1}}D_{21} & \cdots & \sqrt{\tau_7}D_{27} \end{bmatrix}; \quad \Gamma_\tau = \tilde{D}_2\tilde{D^T}_2.$$

The original control problem is to stabilise the uncertain system via the robust control. However, introducing $\tau_1,\ldots,\tau_k$, the problem of absolutely stabilizing an uncertain system becomes equivalent to an output feedback H_∞ control problem, the solution of which is well known [11]. The solutions of the above Riccati equations should satisfy the following conditions to guarantee the closed loop stability: $X > 0$, $Y > 0$ and the spectral radius of the matrix XY is $\rho(XY) < 1$.

The uncertain system (15)-(17) is required to satisfy the following assumptions. Let matrices B_2, C_1, D_1, D_2, G and Γ be defined by

$$B_2 = \begin{bmatrix} B_{20} & \cdots & B_{27} \end{bmatrix}; \quad D_2 = \begin{bmatrix} D_{20} & \cdots & D_{27} \end{bmatrix};$$

$$C_1 = \begin{bmatrix} C_{10} \\ \cdots \\ C_{17} \end{bmatrix}; \quad D_1 = \begin{bmatrix} D_{10} \\ \cdots \\ D_{17} \end{bmatrix}; \quad G = \sum_{k=0}^{7} D'_{1k}D_{1k};$$

$\Gamma = \sum_{k=0}^{7} D'_{2k}D_{2k}$. With the above choice, the pair (A,B_1) is stabilisable, $G > 0$, $\Gamma > 0$, the pair (A,C_2) is detectable, the pair $(A - B_1G^{-1}D'_1C_1, (I - D_1G^{-1}D'_1)C_1)$ is observable, and the pair $(A - B_2D'_2\Gamma^{-1}C_2, B_2(I - D_2\Gamma^{-1}D'_2))$ is controllable. The output-feedback controller is [17]:

$$\dot{x}_c = A_c x_c(t) + B_c y(t), \quad u(t) = C_c x_c(t), \tag{21}$$

where

$$A_c = A + B_1C_c - B_cC_2 + (\tilde{B}_2 - B_c\tilde{D}_2)\tilde{B}'_2X, \tag{22}$$

$$B_c = (I - YX)^{-1}(Y\tilde{C}_2 + \tilde{B}_2\tilde{D}'_2)\Gamma_\tau^{-1}, \tag{23}$$

$$C_c = -G_\tau^{-1}(B'_1X + D'_\tau C_\tau). \tag{24}$$

VI. Controller Design and Performance

First we carry out several simulations by applying large disturbances to get an estimate the operating region during LVRT transients. The controller is designed in the following way to ensure stablity in the operating range of interest:

(i) For a given equilibrium point, obtain matrices for the system representation (15)–(17) according to the procedure outlined in Section IV.
(ii) Choose an operating range $(x^{*p} - x^p)$ $p = 1,\ldots,8$;
(iii) Determine the maximum value of α_k, $k = 0,\ldots,7$, over all values of L and M in this range;
(iv) Design a robust controller given by (21)–(24);
(v) If the controller is feasible, go to step (vi), otherwise stop.
(vi) Increase the range $(x^{*p} - x^p)$ and go to step (ii);

The process described above enables the selection of the largest range for which a feasible controller is obtained. The equilibrium point for this system is ($s_{i0} = 0.013$, $E_{dri0} = 0.2186$, $E_{qri0} = 0.9176$, $V_{dc0} = 1.3$, $V_{tm0} = 1$) pu, $i = 1,2$. For the given power system model, we get the value of α_k given in Table II, for the range of $|s_i^* - s_{i0}| = 0.45$, $|E_{dri}^* - E_{dri0}| = 0.27$, $|E_{qri}^* - E_{qri0}| = 0.28$, $|\delta_i^* - \delta_{i0}| = 66.25^0$, $|V_{dc}^* - V_{dc0}| = 0.35$, $|V_{tm}^* - V_{tm0}| = 0.45$, $|K^* - K_0| = 0.27$, and $|\alpha^* - \alpha_0| = 45^0$, $i = 1,2$. For this problem, $\tau_1 = 0.0005$, $\tau_2 = 0.0106$, $\tau_3 = 0.0346$, $\tau_4 = \tau_5 = \tau_6 = \tau_7 = 0.0045$.

TABLE II
VALUES OF α_k, $k = 0,\ldots,7$.

α_0	α_1	α_2	α_3	α_4	α_5	α_6	α_7
0.85	0.95	0.45	0.98	0.68	0.65	0.79	0.94

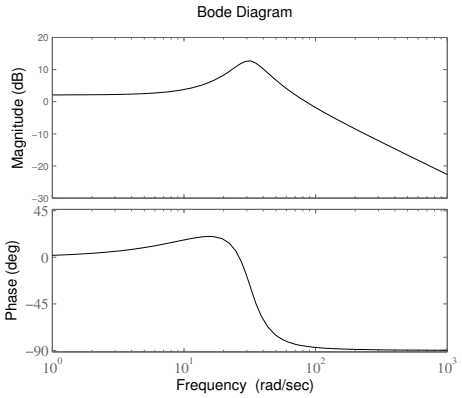

h

Fig. 3. Bode plot of the open loop system.

Figures 3 and 4 show the open loop and closed loop frequency response of the test system. It can be seen from Fig. 3 that there is a resonance peak in the magnitude response in open loop system and also a sharp drop of the phase angle. The closed loop system shown in Fig 4 has higher damping ratio and smaller overshoot.

The performance of the proposed controller for a 500 MVA STATCOM is evaluated for a three phase fault at one of the parallel lines between Bus 6 and Bus 7. The CCT and critical slip CS with the proposed control are 0.18s and 0.215 pu, respectively. To compare the performance, we also determine CCT and CS with PI based STATCOM, which

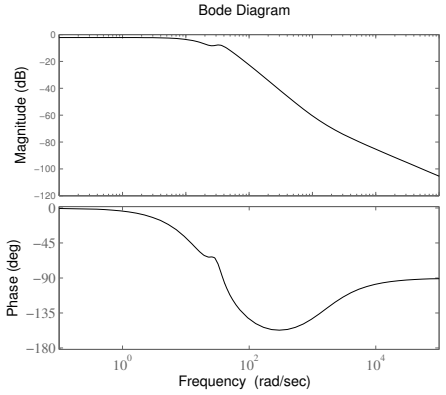

h

Fig. 4. Bode plot of the closed loop system.

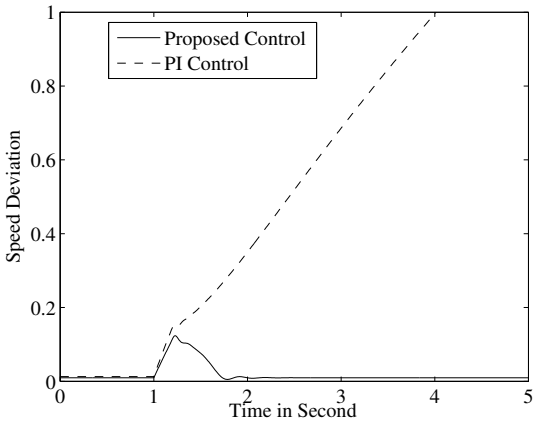

Fig. 5. Generator Speed for the three-phase fault.

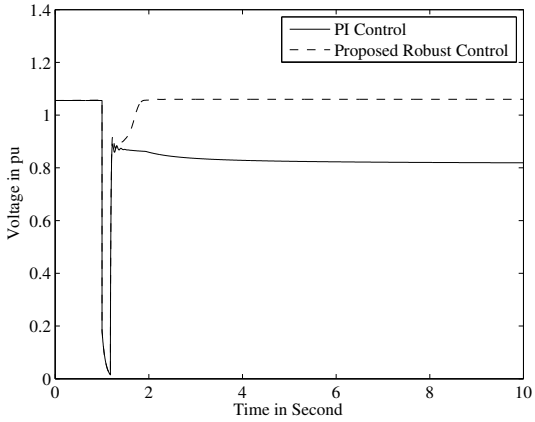

Fig. 6. Voltage at Bus 4 for the three-phase fault.

are 0.165s and 0.19 pu. Figs. 5 and 6 show the speed and terminal voltage of induction generator with the PI controller and the proposed controller, respectively. The fault is applied at $t = 1s$ and cleared at $t = 1.18s$. From Figs. 5 and 6 it is clear that the proposed controller can stabilize the voltage and speed of the induction generator with fault clearing time of 0.18s. The slip of 0.195 pu at the fault clearing is greater than the critical slip of 0.19 pu as obtained for the PI controller with numerical simulations. Thus with PI controller the speed continues to increase even after the fault is cleared. Furthermore, the voltage gradually decreases and the wind generators have to be disconnected from the grid to protect them and avoid voltage collapse. The designed controller guarantees stability if the system operating point, after the fault is cleared, falls within the region for which the controller is designed. We can conclude that the proposed controller performs better than the PI controller and results in a higher critical clearing time.

VII. Conclusions

In this paper an algorithm to design a robust output feedback STATCOM controller is proposed. Detailed modeling of each component and a suitable control strategy of STATCOM is presented. The STATCOM controller scheme is based on the reformulation of the nonlinear dynamics of wind generators using the mean-value theorem. The effectiveness of the proposed control system is verified by applying a large disturbance. The performance of the proposed STATCOM controller is compared with a PI-based STATCOM and simulation results confirm the efficacy of the proposed controller over the conventional STATCOM controller.

References

[1] T. Ackermann, *Wind Power in Power Systems*. England: John Wiley and Sons, Ltd, 2005.

[2] C. Banos, M. Aten, P. Cartwright, and T. C. Green, "Benefits and control of STATCOM with energy storage in wind power generation," in *8th IEE International Conference on AC-DC Power Transmission*, March 2006.

[3] D. Bary, "Increasing renewable accessibility in ireland," in *9th World Energy Congr.*, vol. 1, September 2004, pp. 1–10.

[4] A. Feijo, J. Cidrs, and C. Carrillo, "Third order model for the doubly-fed induction machine," *Electric Power System Research*, vol. 56, pp. 121–127, 2000.

[5] L. Fernndeza, C. Garcaa, J. Saenza, and F. Juradob, "Equivalent models of wind farms by using aggregated wind turbines and equivalent winds," *Energy Conversion and Management, Elsevier*, vol. 50, no. 3, pp. 691–704, 2009.

[6] M. J. Hossain, H. R. Pota, V. Ugrinovskii, and R. A. Ramos, "Excitation control for large disturbances in power systems with dynamic loads," in *IEEE Power Engineering Society General Meeting*, Calgary, Canada, July 2009, pp. 1–6.

[7] R. Itoh and K. lshizaka, "Series connected PWM GTO current/source convertor with symmetrical phase angle control," in *IEE Proceedings*, vol. 137, no. 4, July 1990, pp. 205–212.

[8] C. Jauch, S. M. Islam, P. Srensen, and B. B. Jensen, "Design of a wind turbine pitch angle controller for power system stabilisation," *Renewable Energy, Elsevier*, vol. 32, pp. 2334–2349, 2007.

[9] H. K. Khalil, *Nonlinear Systems*. Macmillan, New York: Prentice-Hall, 1992.

[10] P. Kundur, *Power System Stability and Control*. New York: McGraw-Hill, 1994.

[11] S. R. Moheimani, A. V. Savkin, and I. R. Petersen, "A connection between H_∞ control and the absolute stabilizability of discrete-time uncertain linear systems," *Automatica*, vol. 31, no. 8, pp. 1193–1195, 1995.

[12] M. Molinas, J. A. Suul, and T. Undeland, "Low voltage ride through of wind farms with cage generators: STATCOM versus SVC," *IEEE Trans. on Power Electronics*, vol. 23, no. 3, pp. 1104–1117, 2008.

[13] K. Nandigam and B. H. Chowdhury, "Power flow and stability models for induction generators used in wind turbines," in *Power Engineering Society General Meeting, 2004, IEEE*, vol. 2, June 2004, pp. 2012–2016.

[14] I. R. Petersen, V. A. Ugrinovskii, and A. V. Savkin, *Robust Controller Design Using H_∞ Methods*. London: Springer, 2000.

[15] L. Qi, J. Langston, and M. Steurer, "Applying a STATCOM for stability improvement to an existing wind farm with fixed-speed induction generators," in *Power and Energy Society General Meeting*, July 2008, pp. 1–6.

[16] W. Qiao, G. Venayagamoorthy, and R. Harley, "Real-time implementation of a STATCOM on a wind farm equipped with doubly fed induction generators," in *41st IAS Annual Meeting on Industry Applications*, Oct. 2006.

[17] A. V. Savkin and I. R. Petersen, "Nonlinear versus linear control in the absolute stabilisability of uncertain linear systems with structured uncertainty," *IEEE Trans. on Automatic Control*, vol. 40, no. 1, 1995.

[18] C. Shen, Z. Yang, M. L. Crow, and S. Atcitty, "Control of STATCOM with energy storage device," in *IEEE Power Eng. Soc. Winter Meeting Conf.*, January 2000, pp. 2722–2728.

[19] J. Sun, D. Czarkowski, and Z. Zabar, "Voltage flicker mitigation using PWM-based distribution STATCOM," in *Proceedings of the IEEE Power Engineering Society Summer Meeting*, July 2002.